JOURNAL OF CATALYSIS 135, 481–504 (1992)

Piperidine Hydrogenolysis on a Commercial Hydrocracking Catalyst

III. The Effects of Zeolite Unit Cell Size, Catalyst Sulfur Content, and Coke Deposition on Catalyst Activity and Deactivation

G. C. HADJILOIZOU,[1] J. B. BUTT,[2] AND J. S. DRANOFF

Department of Chemical Engineering, Northwestern University, Evanston, Illinois 60208

Received May 24, 1991; revised December 10, 1991

A group of fresh, deactivated, and deactivated–regenerated commercial hydrocracking catalysts was characterized using piperidine hydrogenolysis as a probe reaction at 301°C, hydrogen partial pressures of about 16 atm, and initial concentrations of piperidine ranging from 4.14×10^{-3} to 11.86×10^{-3} g mol/liter. The first part of the study examined the effects of the zeolite unit cell size on the piperidine hydrogenolysis activity and catalyst deactivation and revealed that over the range of unit cell size examined (24.35–24.56 Å), adsorption equilibrium constants associated with the acidic and metallic catalyst functions decreased while reaction rate constants increased with increasing unit cell size. The increase of acidic function activity with unit cell size is explained in terms of the total number of potential acid sites present per unit cell. The increase of metallic function activity with unit cell size is suggested to reflect mostly changes of the metallic function upon regeneration. Different types of sites are proposed to exist on the metallic catalyst function in order to account for the results. An inverse relationship between catalyst deactivation and unit cell size was generally observed for both catalyst functions. These results point to the zeolite unit cell size as a possible parameter for correlating catalytic activity as well as selectivity, especially for the acidic catalyst function. The second part of the study examined the effects of wt% sulfur and wt% carbon at low levels of sulfur and coke on the piperidine hydrogenolysis activity and showed that the regenerated catalysts with constant zeolite unit cell size (~24.40 Å) and low levels of coke (<0.8 wt%) had similar acidic function activities. The acivity correlation of the metallic function on these regenerated catalysts with low levels of sulfur (<0.4 wt%) also indicated the presence of two different types of metal sites. One showed a decrease in activity with increasing sulfur content and a possible dependency on the regeneration procedure while the activity of the other site was invariant. The activity of the metallic and acidic functions of the catalyst was also examined at high levels of sulfur and coke and constant unit cell size. For this study a series of deactivated samples was used. The metallic function activity of these catalysts was found to decrease with the commercial time on stream. Between 2.2 and 2.6 wt% sulfur, the activity of the metallic function decreased linearly with the sulfur content on the catalyst. At higher levels of sulfur (>2.5 wt%) the deactivated catalysts had similar metallic function activities. Between 2 and 6 wt% carbon, the activity of the acidic function decreased linearly with the carbon content on the catalyst. At low levels of coke (<1.5 wt%), the effect of the unit cell size on acidic activity prevailed. The wt% carbon on the deactivated as well as the regenerated catalysts was found to have no effect on the catalyst deactivation rates observed during the reactions.

INTRODUCTION

One of the most significant problems encountered in hydrocracking, as in many other catalytic processes, is the decrease of the catalytic activity with time on stream. This deactivation process affects not only the activity of the catalyst but also the selectivity since the functions of the hydrocracking catalyst deactivate at different rates. Therefore, various regeneration techniques must be applied commercially in an effort to

[1] Present address: Exxon Research and Development Laboratories, P.O. Box 2226, Baton Rouge, LA 70821.

[2] To whom correspondence should be addressed.

0021-9517/92 $5.00

restore the catalyst's original activity and selectivity.

In previous work, the effects of deactivation and regeneration on the performance of a typical commercial hydrocracking catalyst have been investigated using probe reactions to characterize each function of the catalyst separately. The CoMo metallic function was examined using cyclohexene hydrogenation under conditions where the acidic function had been selectively (and reversibly) prepoisoned by ammonia (*1, 2*). The hydrogenation activity of the deactivated catalysts was found to decrease with the time that they had been on stream commercially, and the loss of hydrogenation activity correlated linearly with the weight percent sulfur on the catalysts. It was also concluded that the reason for the incomplete regeneration of the hydrogenation function in practice was a progressive loss of active sites on the metal (or metal sulfide) function during the deactivation–regeneration process, and not a change in the intrinsic nature of the hydrogenation active sites. The acidic function of the same hydrocracking catalyst was then studied using cumene disproportionation as the probe reaction (*3–7*). In this study, it was found that there was an apparent interaction between the unit cell size of the zeolite and the amount of coke on the catalyst that determined the ultimate activity of the catalyst. The data suggested that changes in the zeolite unit cell size of the hydrocracking catalyst can have a significant effect on the rate of cumene disproportionation. The catalyst deactivation rate was also observed to vary with unit cell size. Thus, unit cell size appeared to be a good parameter for correlating catalyst activity and selectivity. For a fixed unit cell size, a linear decrease in the forward rate constant for cumene disproportionation with weight percent carbon on the catalyst was also observed.

More recently, the feasibility of piperidine hydrogenolysis as a probe reaction for simultaneously characterizing both catalyst functions and for determining their possible mutual interactions under reaction conditions was demonstrated (*8, 9*). This latter work has also shown that catalyst deactivation during the experiments was slow enough to permit reproducible extrapolation of the converison data to zero time and accurate estimation of the initial reaction rate parameters. These rate parameters are consistent with a reaction–deactivation model based on separable kinetics and a Langmuir–Hinshelwood Kinetic mechanism involving two adjacently adsorbed piperidine molecules. We have also shown that the effects of initial piperidine concentration and hydrogen partial pressure on both the reaction and catalyst deactivation rates are consistent with the proposed model (*9, 10*).

In the present paper, we examine the importance of the unit cell size of the zeolite component of the hydrocracking catalyst on the initial reaction rate parameters of piperidine hydrogenolysis and on catalyst deactivation. In addition, this paper reports on the effects of catalyst sulfur content and coke deposition resulting from hydrocracking operations on the rate parameters of the probe reaction and catalyst deactivation. The overall effects of deactivation and regeneration on the hydrocracking catalyst are also discussed.

EXPERIMENTAL

The catalyst samples used in this work were commercial hydrocracking catalysts supplied by Amoco Oil Company. These typically contain Co and Mo oxides deposited on a support composed of crystalline aluminosilicates (ultrastable Y zeolite) dispersed in a porous matrix of silica–alumina. Three different catalyst samples examining the effects of zeolite unit cell size were used in the study and are designated as NU-D, 3651-73-R, and NU-C. NU-D is a sample of the fresh hydrocracking catalyst, while the other two are samples of NU-D that have been deactivated under commercial reaction conditions and later regenerated. Some pertinent characteristics of these catalysts are given in Table 1a. It should be noted that

TABLE 1

Characteristics of Catalyst Samples[a] Used in the Experiments to Determine the Effects of (a) Zeolite Unit Cell Size and (b) Sulfur Content and Coke Deposition on Catalyst Activity and Deactivation

Catalyst	Condition[b]	Unit cell size (Å)	Sulfur content (wt%)	Carbon content (wt%)	Surface area (m^2/g)
(a)					
NU-D	f	24.56	0.10	0.11(0.03)[c]	406
3651-73-R	r	24.40	0.24	0.24	309
NU-C	r	24.35	0.24	0.21	277
(b)					
3651-171-B	r	24.39	0.36	0.067	272
3651-73-R	r	24.40	0.24	0.24	309
4808-54	r	24.41	0.19	0.75	298
NU-E	d	24.45	2.75	2.77	232
3651-9-3	d	24.45	3.04	3.45	—
3651-73	d	24.45	3.45	4.70	260
NU-B	d	24.40	2.41	2.41	211
NU-F	d	24.39	2.53	4.76	200
3651-171-A	d	24.39	3.56	5.48	207
NU-A	d	24.50	2.23	4.00	169

[a] These and other characterization data were supplied by Amoco Oil Company, Searle Laboratories (Illinois), and Galbraith Laboratories (Tennessee) (*8*).

[b] f, Fresh sample, r, regenerated sample; d, deactivated sample.

[c] Results from different laboratories.

these catalysts have very similar sulfur and carbon contents but significantly different unit cell size dimensions, considering the accuracy of such measurements (±0.01 Å). Two other sets of catalyst samples were used in the work to determine the effects of sulfur content and coke deposition. Both sets consist of samples of the fresh hydrocracking catalyst (NU-D) that have already been deactivated under commercial reaction conditions. However, the catalysts in the first set were later regenerated, while those in the second set were not. Some pertinent characteristics of these catalysts are given in Table 1b. In addition, the various regeneration techniques used are described in Table 2. The origin of each of the regenerated samples along with the regeneration techniques employed are listed in Table 3.

All the catalyst samples were crushed and screened to 0.2 mm average particle size and pretreated according to one of two standard methods. In method I*, the catalyst was purged with nitrogen at room temperature for 1 h and then heated to 365°C and held at 365°C for 1 h under a flow of nitrogen. A mixture of 10% H_2S in H_2 was then passed through the catalyst bed at 40 cc/min (STP) and 365°C until the ratio of the mass of the catalyst to the mass of the H_2S passed was equal to unity. The catalyst was then cooled to room temperature under a flow of hydrogen for 1 h. Method III was the same as method I* except the H_2S/H_2 sulfiding step was omitted and the catalyst was cooled in nitrogen instead of hydrogen.

The experiments were conducted in a continuous-flow fixed-bed reactor system at 301°C, about 16 atm hydrogen partial pressure, and initial concentrations of piperidine ranging from 4.14×10^{-3} to 11.86×10^{-3} g mol/liter. Space velocities were in the range of 1.07 to 3.57 h^{-1}. All the experiments were performed without H_2S or a sulfur compound in the feed. Further details of the experimental equipment and procedures as

TABLE 2

The Catalyst Regeneration Techniques

I. Sample NU-B was placed in a muffle furnace and regenerated by oxidation in air, starting at 260°C and ending at 520°C.
II. Catalyst 3651-73 was placed in a muffle furnace and regenerated by oxidation in air ending at 510°C. The procedure is similar to technique IV, except a thicker bed, i.e., a deep bed may have been used.
III. Catalysts were regenerated by Filtrol Corporation using a Roto-Louvre drier. More uniform temperatures were obtained and better gas–catalyst mixing took place.
IV. Catalyst 3651-171-A was placed in large screen baskets in thin layers, i.e., not a deep bed, and was regenerated by oxidation in air starting at 450°F. The temperature was increased as follows: (1) 550°F, 1 h, (2) 650°F, 1 h, (3) 750°F, 1 h, (4) 850°F, 1 h, and (5) 950°F, 2 h.

well as product distribution are given elsewhere (*8, 9*).

RESULTS AND DISCUSSION

Reaction and Deactivation Kinetics

During the piperidine hydrogenolysis kinetic experiments catalyst deactivation occurred; therefore, a reproducible and accurate means of determining fresh catalyst activity data was developed (*8, 9*). In particular, the catalyst samples were compared using:

(a) the kinetic parameters k_i^o, $k_i^{o\prime\prime}$, and K_{pip_i} estimated as follows: (1) obtain initial conversion data by using a catalyst decay correlation (Eq. (1) below), (2) fit the total conversion versus time on stream data to the reaction–deactivation model depicted by Eqs. (2) and (3), and (3) apply Eqs. (4) and (5) for product i,

(b) the decay parameters, a_i, estimated by using Eq. (1), and

(c) the deactivation parameters k_{d_t} and n^* estimated by using Eqs. (2) and (3), where i stands for *N*-*n*-pentylpiperidine **(2)**, 2-*n*-pentylpiperidine **(3)**, or decahydroquinolines **(4)**.

$$x_i(t) = x_i(0)\exp(-a_i t^{0.5}) \tag{1}$$

$$\frac{1}{k_t^o \tau} + \frac{k_{d_t}^* t}{k_t^o \tau} = \left(\frac{1 - x_t}{x_t}\right) \tag{2}$$

$$k_{d_t}^* = k_{d_t}(C_{l_o})^{n^*} \tag{3}$$

$$k_i^o = \frac{x_i^o}{x_t^o} k_t^o \tag{4}$$

$$r_i = k_i^o C_l^2 s_i = \frac{k_i^{o\prime\prime} K_{\text{pip}_i}^2 C_l^2 s_i}{(1 + K_{\text{pip}_i} C_{l_o})^2}. \tag{5}$$

Equation (1) is a modified form of the Voorhies correlation (*11*) while Eqs. (2) and (3) are a reaction–deactivation model based on separable kinetics (*9*). Equations (4) and (5) were derived for the piperidine hydrogenolysis reaction system (*9*). The parameters of these correlations have been estimated by a linear regression method (*8, 9*).

Figure 1 shows a simplified reaction scheme proposed for the hydrogenolysis of piperidine on the commercial hydrocracking catalyst (*9*) that accounts for the formation of the major products **(2, 3,** and **4)** observed in this work. Under the established experimental conditions, it was demonstrated that the piperidine hydrogenolysis reaction exhibits the desired property of bifunctionality. In particular, the formation of products **2** and **3** can be attributed exclusively to the metallic catalyst function (CoMo) while the acidic catalyst function (support) is mainly responsible for the formation of product **4** (*9*).

TABLE 3

Description of the Regenerated Catalysts

Catalyst	Origin	Regeneration technique
NU-C	NU-B	I
3651-73-R	3651-73	II
4808-54	NU-D[a]	III
3651-171-B	3651-171-A	IV

[a] Deactivated catalyst similar to NU-D.

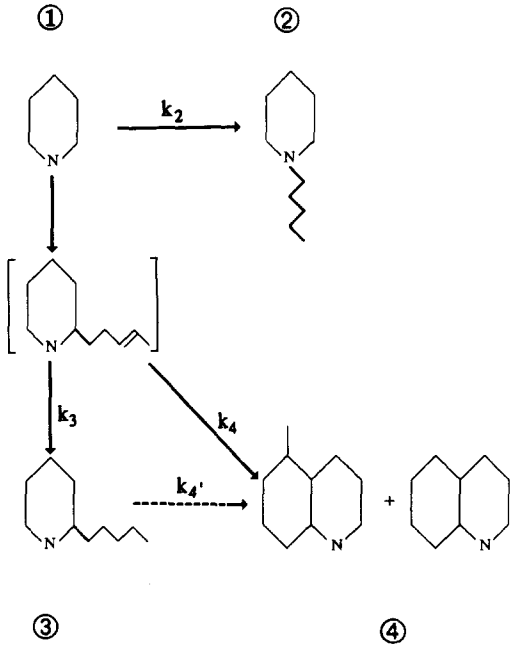

FIG. 1. A simplified reaction scheme for piperidine hydrogenolysis over the commercial hydrocracking catalyst.

Unit Cell Size Effects

Experiments were carried out with the catalysts NU-D, 3651-73-R, and NU-C to examine the importance of the unit cell size (UCS) of the zeolite component of the hydrocracking catalyst on the initial reaction parameters of piperidine hydrogenolysis and on catalyst deactivation. All three catalysts were presulfided according to standard method I*. Table 4 presents the estimated values of the initial reaction rate constants, k_i^o, for the formation of products **2, 3,** and **4,** as calculated using Eq. (4). Examination of the results in Table 4 reveals no indicative change of the initial rate constants with UCS over the range of initial concentrations of piperidine employed. It should be pointed out, however, that the rate constants k_i^o are not the intrinsic rate constants for each reaction step, but rather they represent average parameters, in which for example, changes of the adsorption equilibrium coefficients (changes in the nature of the sites) are included (Eq. (5)). To examine variations of the intrinsic rate constants ($k_i^{o\prime\prime}$) with UCS, the effect of the initial concentration of piperidine on the initial individual reaction rate constants for the three catalysts was studied further using Eq. (5) expressed in terms of products **2, 3,** and **4.** The results are listed in Table 5, where the average deviation values, D, reveal that in each case good agreement between the model, Eq. (5), and the experimental data is observed. Some interesting trends can be observed for the parameters listed in Table 5. In particular, the rate constants $k_i^{o\prime\prime}$ for both products **2** and **4** were found to decrease, while their corresponding adsorption equilibrium constants increased with decreasing UCS. The kinetic parameters associated with product **3** were invariant with UCS within experimental error.

Thus, since both K_{pip_2} and K_{pip_4} do change with UCS, the experimental results suggest that over the range of the UCS examined, the nature of the sites active for the formation of products **2** and **4** does change. If the Langmuir–Hinshelwood reaction mechanism proposed previously (*9*) is used as the actual model, then it was shown that

$$k_{ij}^{o\prime\prime} = k_{ij}^{*\prime} N_{ij}^{o2}, \qquad (6)$$

where N_{ij}^o is the total number of sites active for the formation of product i at time on stream zero on catalyst j. Since the nature of the active sites for products **2** and **4** changes, $k_{ij}^{*\prime}$ for these products is not constant from catalyst to catalyst. In addition, the number of sites may also change from catalyst to catalyst resulting in an overall change in $k_i^{o\prime\prime}$ with UCS. The small differences in wt% S and wt% C between the above catalysts are not expected to contribute much to the observed results, as discussed below.

To determine the effect of UCS on catalyst deactivation, the decay parameter a_i associated with the formation of products **2, 3,** and **4** was estimated for the above catalysts using Eq. (1). The estimated values of a_i are plotted as a function of UCS for each of

TABLE 4

The Effect of UCS on k_i^o at Different Initial Concentrations of Piperidine at 301°C

Experiment	$C_{I_o} \times 10^3$ (g mol/liter)	Catalyst[a]	UCS (Å)	k_2^o	k_3^o (liter^2/g mol/g cat/min)	k_4^o
52	4.14	NU-D	24.56	3.32	2.09	1.64
61	4.21	3651-73-R	24.40	3.30	1.98	1.66
60	4.20	NU-C	24.35	4.07	1.75	1.95
56	8.11	NU-D	24.56	1.96	1.02	0.826
63	8.09	3651-73-R	24.40	1.71	1.12	0.797
62	8.10	NU-C	24.35	1.58	1.10	0.755
59	11.84	NU-D	24.56	1.30	0.663	0.607
65	11.86	3651-73-R	24.40	1.08	0.637	0.436
64	11.84	NU-C	24.35	1.02	0.615	0.433

[a] See Table 1a.

the three initial piperidine concentrations in Figs. 2 through 4. It generally appears that the catalyst deactivation rate varies inversely with zeolite UCS. Deviations from this conclusion are observed, especially at the highest initial concentration of piperidine (~12×10^{-3} g mol/liter) where deactivation effects due to the adsorbed nitrogen compounds (*10*) are probably interfering with the effects due to UCS variation.

The effect of the initial concentration of piperidine on the total apparent deactivation rate constant, $k_{d_t}^*$, was also examined for the three catalysts using Eq. (3). The results are listed in Table 6. For all catalyst samples the deactivation order with respect to the initial concentration of piperidine is about 1. The observed variation of k_{d_t} with UCS is either due to the lumping of the different individual deactivation reaction steps occurring on both catalyst functions or due to the fact that terms such as k'_{d_t} and E_{d_t}, which are included in k_{d_t} (Eq. (7)) may be changing in a different way with UCS. In order to check the latter possibility, a more extensive set of data is required than that reported here for analysis of the temperature dependence of k_{d_t}. Overall Eq. (3) managed to fit the data satisfactorily as indicated by the values of R^2.

$$k_{d_t} = k'_{d_t} \exp\left(-\frac{E_{d_t}}{RT}\right). \tag{7}$$

The above results suggest that upon de-

TABLE 5

The Effect of UCS on $k_i^{o\prime\prime}$ and K_{pip_i} at 301°C

Reaction parameter[a]	NU-D UCS = 24.56 Å	D (%)	3651-73-R UCS = 24.40 Å	D (%)	NU-C UCS = 24.35 Å	D (%)
$k_2^{o\prime\prime} \times 10^4$	5.47	0.55	3.46	0.56	2.36	5.6
K_{pip_2}	115.6		164.7		274.0	
$k_3^{o\prime\prime} \times 10^4$	2.05	2.1	1.99	4.0	2.17	6.0
K_{pip_3}	170.7		177.4		151.2	
$k_4^{o\prime\prime} \times 10^4$	2.35	5.2	1.08	2.5	0.901	2.1
K_{pip_4}	123.1		265.7		375.1	

[a] $k_i^{o\prime\prime}$ in g mol/g cat/min, K_{pip_i} in liter/g mol.

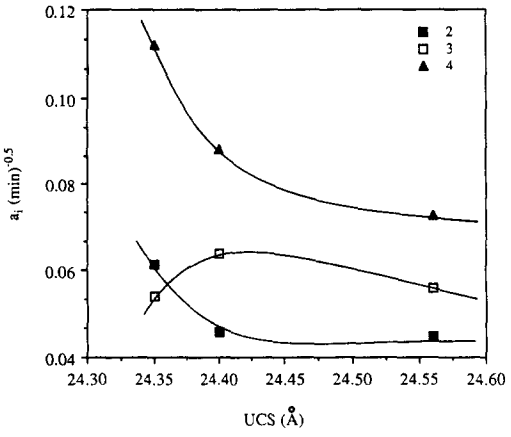

FIG. 2. The effect of unit cell size on a_i at an initial piperidine concentration of about 4×10^{-3} g mol/liter and 301°C.

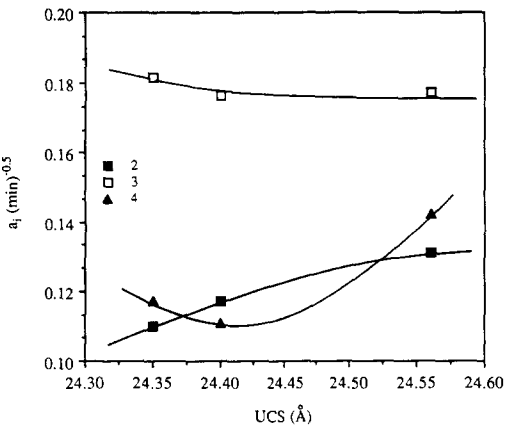

FIG. 4. The effect of unit cell size on a_i at an initial piperidine concentration of about 12×10^{-3} g mol/liter and 301°C.

alumination (decreasing the unit cell size), the catalytic activity and selectivity are changed. This points to the UCS as a possible parameter for measuring catalytic activity as well as selectivity. Originally, Pine *et al.*(*12*) studied the behavior of various ultrastable Y (USY)-based catalysts in the cracking of a light VGO and attempted to correlate data on zeolite stability as well as catalyst activity and selectivity against the unit cell constant of the catalyst. They found that the gas oil cracking activity increased while the C_3–gas yield and the naphtha research and motor octane decreased with increasing UCS. The catalysts examined had unit cell sizes ranging from 24.23 to 24.34 Å and the experimental data indicated that the UCS determined the catalytic activity and selectivity regardless of what method was used to change it. In view of their experimental results, they concluded that the UCS is an effective correlating parameter in the characterization of the acidity, activity, stability, and selectivity of FCC catalysts. In accordance with the work by Breck and Flanigen (*13*), Pine *et al.* (*12*) assumed that the UCS of a faujasite zeolite is a measure of the Si/Al ratio of the zeolite framework and of the total number of tetrahedral aluminum sites per unit cell (the validity of this

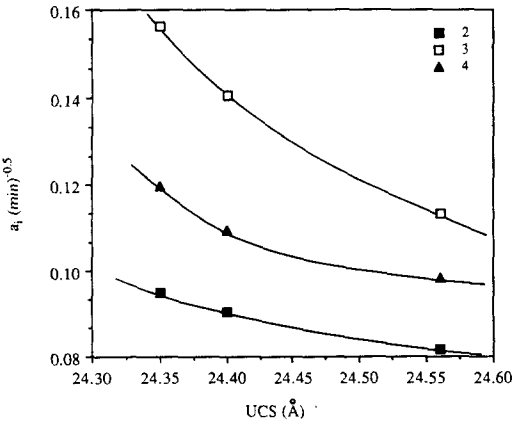

FIG. 3. The effect of unit cell size on a_i at an initial piperidine concentration of about 8×10^{-3} g mol/liter and 301°C.

TABLE 6

The Effect of UCS on k_{d_t} and n^* at 301°C

Catalyst	UCS (Å)	k_{d_t} (liter/g mol/min)	n^*	R^2
NU-D	24.56	0.756	0.894	0.994
3651-73-R	24.40	2.76	1.23	0.977
NU-C	24.35	0.608	0.882	0.952

assumption is examined below). These are considered to be equal to the total number of potential acid sites per unit cell. As the UCS decreases the number of acid sites per unit cell also decreases. Consequently, the acid site density decreases, while the probability of any given acid site becoming more isolated from the other acid sites increases. If it is postulated that the acid strength of a site is determined by its degree of isolation from its neighboring acid sites, then the UCS becomes a measure of the number as well as type of acid sites present in the zeolite crystal structure (*12*).

A relationship between UCS and catalytic activity was also reported by Absil *et al.* (*7*) during a cumene disproportionation study on these catalysts. Specifically, they observed a maximum in cumene disproportionation activity on the USY zeolite-containing catalysts at a Si/Al ratio between 5.2 and 9.5, which corresponds to a SiO_2/Al_2O_3 ratio between 10.4 and 19.0. Previous experimental studies in the literature have also reported maxima in catalytic activity with increasing Si/Al ratios or decreasing UCS (*14–18*). However, this activity maximum was not observed in the results of the present study. Similarly, Jiao *et al.* (*19*) found that the catalytic activity of USY zeolites in the cracking of cumene decreased as the Si/Al ratio increased. No activity maximum was reported. Finally, in a recent study, Gao *et al.* (*20*) examined the activities of a series of dealuminated Y zeolites toward cumene cracking and *n*-propanol dehydration and reported a maximum of the dealkylation activity and a continuous decrease of the dehydration activity with increasing Si/Al ratio. Considering that these are typical strong-acid-catalyzed and weak-acid-catalyzed reactions, respectively, their results agreed well with strong and total surface acidity measurements, if one assumes that nearly all the zeolite acid sites can function in the dehydration reaction (*20*). Thus, depending on the type of zeolite acidity needed for a chemical transformation, variation of the zeolite structure may have different effects in catalytic performance.

In their work, Pine *et al.* (*12*) also concluded that the decrease in octane number as UCS increased was due to a higher acid site density, which allowed hydrogen transfer and resulted in a more paraffinic product. Thus, decreasing the UCS of the zeolite and in effect lowering the acid site density decreased hydrogen transfer, which led to a more olefinic naphtha. By analogy, it would also be expected that the catalyst deactivation rate should vary inversely with zeolite UCS since the decrease in hydrogen transfer reactions and the production of more olefins at decreasing unit cell constants would favor coke formation, thus increasing catalyst deactivation. This was indeed observed in the present work where the decay parameter a_i for the three major products **(2, 3,** and **4)** was found to vary inversely with the zeolite UCS over most of the initial piperidine concentration range of the experiments (Figs. 2–4).

An inverse relationship between catalyst deactivation and UCS has also been reported in other studies (*7, 18*). Specifically, Arribas *et al.* (*18*) examined the cracking of vacuum gas oil on Y zeolites dealuminated by different procedures and found that for zeolite samples that were deep-bed calcined at 550°C after cation exchange, with unit cell dimensions in the range of 24.40 to 24.70 Å, the selectivity to coke increased with decreasing UCS. Note that catalyst 3651-73-R (and possibly NU-C), used in the present work, was produced by regeneration using a deep-bed technique at temperatures up to 510°C (Tables 2 and 3). Thus, by comparison, an agreement can be seen between the results with the deep-bed samples of Arribas *et al.* (*18*) and the results of this study, in that coke formation or catalyst deactivation rate varies inversely with UCS.

In another study, Corma *et al.* (*21*) examined the influence of the nature and amount of basic nitrogen compounds in the feed on the activity and selectivity of a series of ultrastable Y zeolites during *n*-heptane

cracking at atmospheric pressure and 430°C. They reported that the decay of the catalysts due to poisoning by a fixed amount of basic nitrogen in the feed decreased first with dealumination, reached a minimum at about 24 Al^{3+} ions per unit cell (i.e., a framework Si/Al ratio of about 7), and then increased sharply with further dealumination. These results indicated that there must have been an increase in the amount of acid sites active for cracking with increasing dealumination, up to about 20 to 30 Al^{3+} ions per unit cell. After this point, further dealumination leads to a decrease in the number of active sites. If the correlation proposed by Fichtner-Schmittler *et al.* (*22*) is used to calculate the number of Al ions per unit cell for the catalysts employed in the present work, then values of 37, 19, and 13 Al/u.c. are obtained for NU-D, 3651-73-R, and NU-C, respectively. The results presented earlier indicated that in general the deactivation rates for the formation of products **2, 3,** and **4** increased with decreasing UCS or decreasing Al/u.c. ($37 < 19 < 13$). Although a direct comparison with the results presented by Corma *et al.* (*21*) cannot be made, it can be seen that within the range of UCS studied, an inverse relationship between catalyst deactivation and UCS has also been observed by others.

From the above discussion the following picture emerges. If the Si/Al ratio is taken to be a measure of the total number of potential acid sites per unit cell, then as the Si/Al ratio increases by dealumination, the number of acid sites per unit cell decreases. This would cause the rate constant for the formation of product **4,** which is attributed to the zeolite part of the catalyst (*9*), to decrease with decreasing UCS, as was indeed the case (Table 5). As the UCS decreases the acid sites become more isolated from each other and the acid site strength increases. If the deactivation process is thought to be caused by a nitrogen compound that deposits on the acid sites of the catalyst and develops into coke-like products (*10*), which also cover the hydrogenation sites adjacent to the acid sites, then the acid strength of the sites becomes an important factor in the first step of coke formation, i.e., irreversible adsorption of the coke precursor molecule. Thus, increasing the acid site strength increases catalyst deactivation. The increase in the decay parameter a_i, of products **2, 3,** and **4,** with decreasing UCS is in agreement with the above proposal.

The adsorption equilibrium constant for product **4** was also found to change with UCS (Table 5). Decreasing the UCS, i.e., increasing the acid site strength resulted in an increase in K_{pip_4}. If K_{pip_i} is expressed in the form

$$K_{\text{pip}_i} = K'_{\text{pip}_i} \exp[-\Delta H_{\text{pip}_i}/\text{RT}], \qquad (8)$$

then $(-\Delta H_{\text{pip}_i})$, as a first approximation, is an average measure of the adsorptive properties of the sites active for formation of product i. Furthermore, K'_{pip_i} is proportional to the number of sites active for adsorption of reactant molecules. Thus, a large value of K_{pip_i} implies strong bonding on the catalyst surface. Based on this definition, the increase in K_{pip_4} with decreasing UCS is expected since the increasing acid site strength will result in stronger bonding between reactant molecules and the catalyst surface.

The decrease in the initial rate constant for product **2,** $k_2^{0\prime\prime}$, when going from NU-D to 3651-73-R to NU-C (Table 5), does not reflect a direct correlation with UCS since this product is attributed to the metallic catalyst function (*9*). It rather indicates that regeneration by simple coke/sulfur burning was unable to fully restore the activity of the metal function sites responsible for forming product **2.** This is in agreement with the ESCA results for these catalysts reported by Pookote *et al.* (*1, 2*), who found that regeneration reduced the surface Mo/Co ratio to a value lower than those of both the fresh and spent catalysts, thus suggesting migration of Mo into the bulk. Similarly, the increase of the adsorption equilibrium constant for product **2,** K_{pip_2}, with decreasing UCS (Table 5) cannot be simply ex-

plained with the increase of the acid site strength of the zeolite, because this product is formed on the metallic function of the catalyst. Although the exact preparation technique for these catalysts is proprietary information, it can be speculated that perhaps the proximity of the zeolite acid sites to the metal sites, responsible for the formation of product **2,** is the reason for the observed change in K_{pip_2}. In particular, as the UCS decreases and the zeolite acid sites are becoming more isolated from each other and stronger, at the same time the metal acid sites that participate in the formation of product **2** are also becoming more isolated (from the zeolite acid sites) and stronger, resulting in an increase of K_{pip_2}. Even though this is purely a speculation, it appears to be consistent with the above discussion and results.

The observed invariance in the parameters for product **3** with respect to changes in the UCS of the zeolite, although in agreement with the assignment of this product to the metallic catalyst function (*9*), does not agree with the results found for product **2,** which is also attributed to the metallic function. Obviously, a difference must exist between the metal sites that participate in the formation of products **2** and **3.** Based on literature investigations (*23–27*), the presence of two different types of sites on the metallic function is indeed possible. For example, a different behavior between the active sites for formation of products **2** and **3** was also observed when the catalyst deactivation rate of NU-D was examined as a function of initial concentration of piperidine (*8, 10*). In particular, the decay parameter for the formation of product **3,** a_3, was found to be more sensitive to the piperidine concentration than the corresponding parameter for product **2,** a_2.

If the UCS is assumed to be a measure of the Si/Al ratio of the ultrastable zeolite framework, then the decrease in the UCS suggests that during the deactivation–regeneration process the zeolite is dealuminated. The variation of the UCS upon dealumination of the zeolite framework and the fate of the aluminum thus liberated have been investigated by several literature studies and discussed elsewhere (*5, 7, 8*). The results presented here were explained according to the proposal by Pine *et al.* (*12*) that the UCS is a good measure of the Si/Al ratio of the zeolite in a steamed catalyst. However, other factors in addition to the Si/Al ratio also affect the UCS of a faujasite zeolite. In particular, the UCS of a metal-exchanged ultrastable Y zeolite also depends on the exchanged metals present in the zeolite, and the extra-lattice aluminum produced during the stabilization process. Therefore, the assumption that the UCS is a true measure of the Si/Al ratio of the zeolite framework of a steamed catalyst may not be completely justified. Rabo (*28*) stated that the determination of the framework Si/Al ratio of steam-stabilized Y zeolites based on the X-ray diffraction pattern alone is difficult. During dealumination, the UCS is affected both by silicon enrichment of the framework and by the stuffing of the sodalite cages with aluminum oxide/hydroxide clusters formed when water vapor attacks zeolite aluminum atoms (*29–31*). These two phenomena are expected to contribute to changes in UCS in opposing directions. The effect of extra-lattice aluminum on catalytic activity was examined by Jacobs *et al.* (*32*) by preparing ultrastable Y catalyst samples both treated and untreated in NaOH to remove the extra-lattice aluminum. The samples obtained had the same UCS within experimental error; however, their initial activities for cumene cracking per hydroxyl group were considerably different. The cracking activity of the untreated sample was higher than that of the NaOH-treated sample. Thus, the extra-lattice aluminum had a favorable effect on the cracking activity. In addition, Sohn *et al.*(*33*) pointed out that the extra-lattice aluminum may also play a role in coke formation and catalyst deactivation. Their results during *n*-hexane cracking experiments indicated that dealuminated zeolites, which contained extra-

lattice aluminum, deactivated more readily than an HY zeolite. Other workers have also recently reported that the unit cell parameter (framework Si/Al ratio) cannot by itself explain the activity and selectivity of dealuminated zeolites (*34*).

The results here are consistent with literature information and can be explained if the UCS is regarded as a measure of the Si/Al ratio of the zeolite framework. However, it should be noted that UCS data alone cannot determine the exact Si/Al ratio, mainly because of the effect of extra-lattice aluminum and possibly other cations on UCS. Furthermore, catalytic activity and selectivity may also be affected by the extra-lattice aluminum.

The Effects of Low Levels of Sulfur and Coke

In the present section the effects of low levels of sulfur and coke on catalytic activity are examined. Since the above results indicated that the zeolite UCS has a profound effect not only on the activity of the hydrocracking catalyst, but also on the nature of the catalytic sites (especially of those associated with the acidic catalyst function), catalyst samples having a similar unit cell dimension were chosen. In particular, three different regenerated catalysts were used: 3651-171-B, 3651-73-R, and 4808-54, as listed in Table 1b. All catalysts were presulfided according to standard method I* and the experiments were conducted at an initial concentration of piperidine of about 4.2×10^{-3} g mol/liter and a space velocity of $1.1\ h^{-1}$.

The initial reaction rate constants, k_i^o, were calculated as explained above and the results are listed in Table 7. Although the difference in the UCS of catalysts 3651-171-B and 4808-54 is slightly larger than the error associated with such measurements, each of these catalysts can be compared with 3651-73-R. Furthermore, Pookote (*1*) demonstrated, using activation energy data for cyclohexene hydrogenation on fresh and regenerated catalysts, that the deactivation–regeneration procedure does not involve chemical alteration of the catalyst metal sites. In addition, previous experiments on regenerated catalysts using cumene disproportionation as the probe reaction (*5*) indicated that the wt% carbon does not affect the nature of the catalyst acidic sites; this conclusion was based on a constant value for the adsorption equilibrium coefficient of cumene. Therefore, as a first approximation it can be assumed that the values of the adsorption equilibrium coefficients, K_{pip_i}, for 3651-171-B, 3651-73-R, and 4808-54 are about the same. Consequently, according to the Langmuir–Hinshelwood kinetic mechanism derived previously (*9*) and represented by Eq. (5), the estimated k_i^o values can be used to examine the above catalysts and to relate any activity variations to changes in the number of sites resulting from either sulfur or coke deposition.

Examination of the results listed in Table 7 indicates that at a constant UCS, the regenerated catalysts with low levels of coke and sulfur have similar activities, within experimental error (*9*), for the formation of product **4,** which is attributed to the acidic catalyst support. The same result is observed for the formation of product **3,** which is attributed to the metallic catalyst function. However, the activity of the metal sites associated with formation of product **2** seems to exhibit a dependency on the wt% sulfur, which was present on the catalysts prior to sulfidation. The above results reveal a difference in the metal sites that participate in the formation of products **2** and **3,** as was also found and discussed in the results above on the UCS effects.

To understand the nature of the catalysts under investigation, their history will next be discussed. The above catalysts were fresh samples that have been used in a commercial hydrocracker for about 2 years and then regenerated by oxidation in air (Tables 2 and 3). Almost all of the fundamental information on regeneration is concerned with the reaction of coke and oxygen. In fixed-bed reactors, the burning takes place largely

TABLE 7

The Effects of Sulfur Content and Coke Deposition on k_i^0 at Constant UCS and Low Levels of Sulfur and Coke[a]

Experiment	Catalyst	S (wt%)	C (wt%)	UCS (Å)	k_2^0	k_3^0	k_4^0
					(liter^2/g mol/g cat/min)		
74	3651-171-B	0.36	0.067	24.39	2.98	1.91	1.52
61	3651-73-R	0.24	0.24	24.40	3.30	1.98	1.66
66	4808-54	0.19	0.75	24.41	4.10	1.71	1.62

[a] Temperature = 301°C; $C_{l_0} \approx 4.2 \times 10^{-3}$ g mol/liter.

within a zone that moves slowly through the reactor, and the temperature along the bed varies greatly with position and time (*35*). During coke removal, oxygen diffuses into the coked catalyst pores where the surface combustion of coke occurs. The relative rates of diffusion and surface reaction dictate whether coke removal is uniform or not. In the former case, the oxygen concentration gradient throughout the pellet is negligible and the coke concentration decreases uniformly throughout the catalyst pellet during the combustion reaction. At sufficiently high temperatures though, the regeneration reaction may become diffusion-limited, and oxygen reacts as fast as it is transported to the carbon. In a spherical catalyst particle, reaction then takes place solely at a spherical interface, which moves progressively to the center. The combustion of carbonaceous deposits within porous silica–alumina catalyst particles in near-spherical bead form under diffusion-controlled kinetics was examined by Weisz and Goodwin (*36*). The carbonaceous material was deposited from a hydrocarbon atmosphere such that it was radially uniform throughout the particle. Examination of the silica–alumina beads revealed that at diffusion-free conditions (temperature <470°C), the coke was uniformly removed from the catalyst. At intermediate diffusion conditions, a progressive darkening toward the center of the bead was visible. Under highly diffusion-controlled regeneration conditions, a black sphere surrounded concentrically by a white or light gray spherical shell from which all the coke has been removed was observed (shell-progressive combustion).

In the case of the catalyst 4808-54, used in the present work, a darkened region in the center of the pellet was indeed found when it was cut in half (*5*). Furthermore, upon grinding pellets of this catalyst, particles in the resulting mixture with colors ranging from black to brown or light gray were observed. Therefore, most likely, the present catalysts have been obtained by diffusion-controlled regeneration of the corresponding deactivated samples.

Absil (*5*) used the same regenerated catalysts as the present investigation and found a linear decrease in the cumene disproportionation activity with wt% carbon. The results were explained assuming the catalysts were regenerated under highly diffusion-controlled conditions. The invariance of rate constants k_3^0 and k_4^0, as reported in Table 7, can be explained considering the results discussed by Hadjiloizou *et al.* (*10*). In particular, the coke formation data indicated that during the hydrogenolysis of piperidine on the fresh catalyst at conditions comparable to the above experiments, carbon as high as 4.78 wt% is deposited at reaction times less than 90 min. The strong poisoning nature of the nitrogen compounds in the system, which eventually leads to rapid coke deposition, results in the inability to observe any changes in catalytic activity with such low levels of sulfur and coke. As discussed next, correlations of activity with wt% sulfur and wt% coke at higher levels of

sulfur and coke have been obtained. The observed variation of k_2^0, as indicated in Table 7, might be due to a higher sensitivity toward sulfur of the metal sites forming product **2** or might even reflect important differences between the regeneration techniques used for these catalysts. For example, catalyst 4808-54, which exhibited the highest activity for the formation of product **2,** was obtained by using a regeneration procedure in which more uniform temperatures were present and better gas–catalyst mixing took place (Tables 2 and 3). Furthermore, one of the problems addressed previously (*1, 2*) is that properly controlled coke burning for regeneration appears to return full activity for the acidic function; however, full metallic function activity is not recovered. Since the regeneration procedure is effective in reducing the sulfur level (Table 1) and the irreversible loss in activity does not involve chemical alteration (*1*), there is apparently loss of available metal surface area in the regeneration. This may account for the inability to restore the metal sites activity by simple coke/sulfur burning and the observed differences in metallic function activities of the regenerated samples, as was also concluded above in the study on the UCS effects.

When comparing the catalysts NU-D, 3651-73-R, and NU-C above on the basis of their UCS, the contribution of the small differences in the low levels of wt% S and wt% C among the catalysts (Table 1a) to the observed results was considered negligible. The experiments in the present section indicate that the small differences between the wt% S and wt% C among the above catalysts are not expected to affect the UCS results obtained for the formation of products **3** and **4.** In addition, although low levels of sulfur were indicated above possibly to affect the value of k_2^0, the decrease in $k_2^{0\prime\prime}$ (Eq. (5)) observed in going from NU-D to 3651-73-R to NU-C (Table 5) cannot be simply explained in terms of sulfur content, since catalysts 3651-73-R and NU-C have the same wt% S but exhibited different activities. However, the higher $k_2^{0\prime\prime}$ value of NU-D could be the result of (a) lower sulfur content on this catalyst and (b) decrease of available metal surface in the regenerated samples.

The Effects of High Levels of Sulfur and Coke

This section deals with the characterization of deactivated catalysts for their metallic and acidic function activities. For the reasons stated above, the deactivated samples were separated into categories according to their unit cell size. The experimental conditions were the same with those employed for the samples with low levels of sulfur and coke; however, a variation of the catalyst pretreatment was used. Since the deactivated (used) catalysts were initially sulfided at hydrocracking conditions, presulfidation is not required. Furthermore, Pookote (*1*) found that presulfiding commercially used catalyst samples lowered the hydrogenation activity of the catalysts. Therefore, the deactivated catalysts were pretreated according to standard method III. This procedure did not alter the sulfur and coke contents of the catalysts. The initial reaction rate constants, k_i^0, for the deactivated catalysts as calculated using Eq. (4) are listed in Table 8. Previous activation energy results of Pookote (*1*) indicated some chemical alteration of the nature of the hydrogenation active sites upon deactivation. Hence, the k_i^0 values can be used as a measure of relative activity for the catalysts but not as an indication of any possible changes in the nature or the number of active sites.

The activity of the metallic catalyst function will be examined first. Based on the previous work using cyclohexene hydrogenation as the probe reaction (*2*) and in view of the results and discussion presented above, the activity of the metallic function is expected to be primarily dependent on sulfur deposition. In addition, Pookote (*1*) reported a correlation between hydrogenation activity and commercial time on stream for deactivated samples. Figures 5 and 6 show the trend of relative activity with time

TABLE 8

The Effects of Sulfur Content and Coke Deposition on k_i^0 at Constant UCS and High Levels of Sulfur and Coke[a]

Experiment	Catalyst	S (wt%)	C (wt%)	UCS (Å)	Time on stream (years)	k_2^0	k_3^0	k_4^0
						(liter^2/g mol/g cat/min)		
67	NU-E	2.75	2.77	24.45	0.25	2.22	0.865	0.851
68	3651-9-3	3.04	3.45	24.45	1.00	1.47	0.867	0.685
69	3651-73	3.45	4.70	24.45	2.00	1.34	0.601	0.411
70	NU-B	2.41	2.41	24.40	1.00	1.65	0.706	1.02
71	NU-F	2.53	4.76	24.39	2.00	1.22	0.558	0.741
73	3651-171-A	3.56	5.48	24.39	2.00	1.20	0.557	0.596
72	NU-A	2.23	4.00	24.50	0.03	2.17	0.840	0.416

[a] Temperature = 301°C; $C_{l_0} \approx 4.2 \times 10^{-3}$ g mol/liter.

on stream for the formation of products **2** and **3,** respectively. Although both plots indicate a linear decrease of the metallic function activity with time on stream, catalysts NU-E and 3651-9-3 are off the correlation. This seems to be a problem associated with point samples, i.e., those removed from only one point in a reactor, as was also concluded in the cyclohexene hydrogenation study (*2*). Sulfur and carbon contents of such catalyst samples reflect localized intrareactor gradients that could vary considerably between bed inlet and bed outlet (*37*) for the same time on stream. Therefore, that measure is not a useful correlating parameter for samples from different points. Much better results are obtained from the composite samples, as shown in Figs. 5 and 6, and in the correlations discussed below. As can be seen in Figs. 5 and 6, overall losses in the metallic function activity are about a factor of 2 and 1.5 for the formation of products **2** and **3,** respectively, for the catalysts that have been on stream for up to 2 years.

The differences in the history of these deactivated catalysts (changes in operating conditions and variations in the feed streams) render activity as a function of commercial time on stream not a valid correlation in many cases. However, examining activity as a function of the catalyst sulfur content might indicate some changes in the

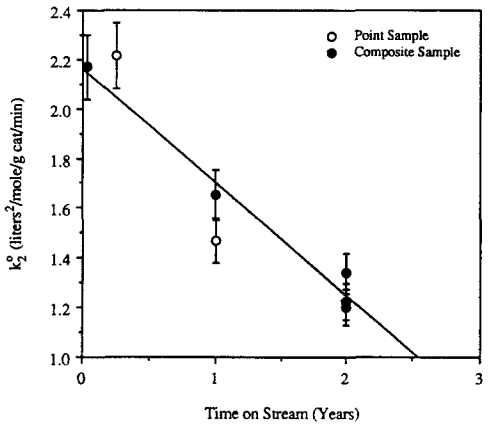

FIG. 5. Plot of k_2^0 versus catalyst commercial time on stream.

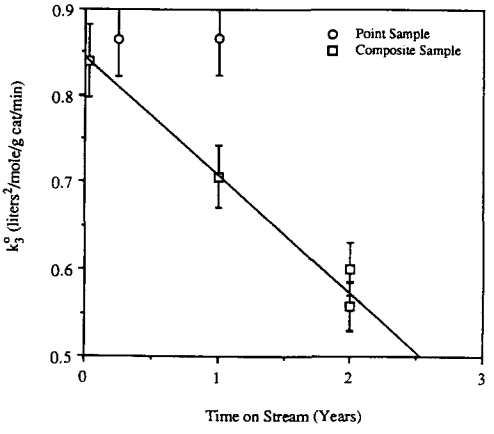

FIG. 6. Plot of k_3^0 versus catalyst commercial time on stream.

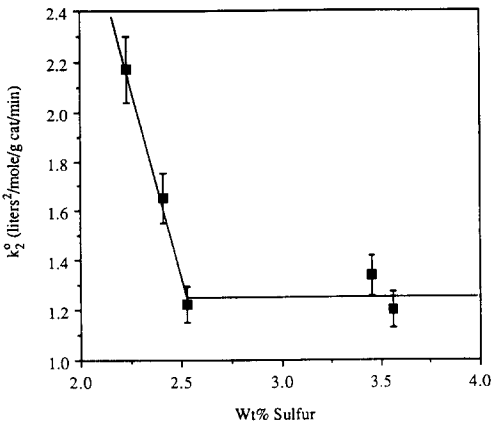

FIG. 7. Plot of k_2^o versus catalyst wt% sulfur.

metal sites of the catalyst. Note that the total amount of sulfur on the catalyst is a combination of surface sulfur, bulk sulfur, and the amount of sulfur trapped in the coke structure. Hence, even this measure does not reflect the exact surface conditions. Nevertheless, as a first approximation, the metallic function activity is correlated with the wt% S on the deactivated catalysts and the results are shown in Figs. 7 and 8 for k_2^o and k_3^o, respectively. In this correlation, samples NU-E and 3651-9-3 again do not follow the general trend, possibly because of the reasons described earlier, and thus they are not included in the analysis. Furthermore, samples with higher than 2.5 wt% S exhibited the same activity for the formation of products **2** and **3,** as shown in Figs. 7 and 8, respectively. Thus, it is apparent that there is a critical weight percent sulfur range over which progressive deposition of sulfur on the catalyst rapidly decreases the activity of the metallic function. After this sharp decrease in activity, deposition of more sulfur on the catalyst surface does not affect catalytic activity. The linear relationships obtained between the sulfur content and the rate constants k_2^o and k_3^o, as illustrated in Figs. 7 and 8, respectively, can be represented by

$$k_2^o = 9.17 - 3.13\,[\text{wt\% sulfur}] \quad (9)$$

(coefficient of determination = 0.996)

$$k_3^o = 2.91 - 0.926\,[\text{wt\% sulfur}] \quad (10)$$

(coefficient of determination = 0.979), where $2.2 < \text{wt\% sulfur} < 2.6$. Although the above correlations seem quite adequate for the catalysts examined, it should be pointed out that in reality, the activity of the metallic function may depend in a complex way on a number of variables such as sulfur content, carbon content, and metals deposition (V, Ni). In the present work there was no correlation between coke on the catalyst and metallic function activity or sulfur on the catalyst and acidic function activity. These results are in full agreement with the previous studies of Pookote *et al.* (*1, 2*) and Absil (*5*).

The inability to correlate the activity of the metallic function with wt% carbon points to the fact that coke formation is primarily associated with deactivation of the acidic function. This is consistent with the model proposed by Beuther and Larson (*38*), which allocates the majority of the coke present on the catalyst to the acidic sites. Thus, coke formation can be nonuniformly distributed on catalysts. Based on various data from characterization of carbon deposits on used reforming catalysts, Franck and Martino (*39*) pointed out that three-dimensional deposits are present on

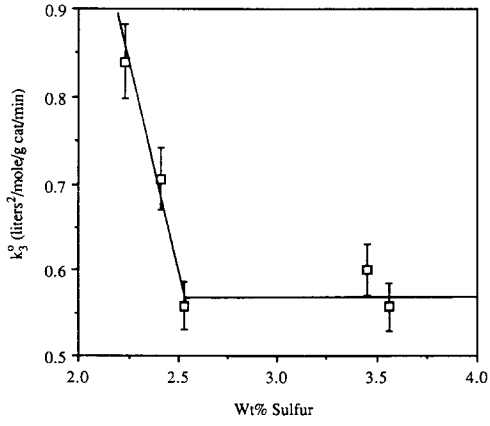

FIG. 8. Plot of k_3^o versus catalyst wt% sulfur.

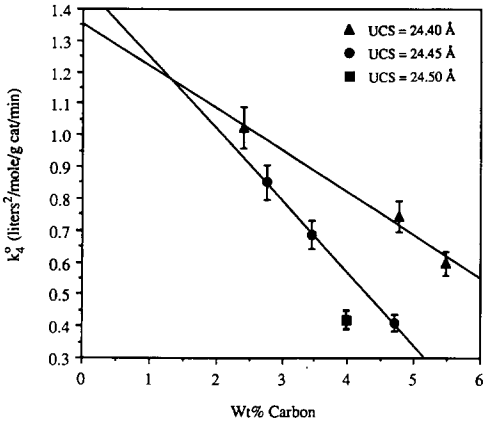

FIG. 9. Plot of k_4° versus wt% carbon for deactivated catalysts.

such catalysts, and even with 20 wt% carbon, some coke-free areas must still remain on the catalyst. Petersen (*40*) reported that the lack of uniformity of coke laydown has indeed been demonstrated by various studies. For example, a direct measure of a nonuniform distribution of coke on a catalyst was carried out by an experiment of Richardson (*41*). He used a spherical cobalt molybdate on alumina catalyst, which was first coked/deactivated and then regenerated under conditions such that mass transfer of oxygen to the carbon was the limiting step in the regeneration reaction. Thus, the model of shell-progressive combustion proposed by Weisz and Goodwin (*36*) (see above) was applicable in this case. The cumulative and local carbon profiles as a function of radial distance were not uniform but exhibited about 9 wt% coke at the exterior and about 1 wt% coke in the interior.

The relative activity of the acidic function, as determined by k_4°, was examined as a function of wt% carbon for the two sets of catalysts with constant UCS shown in Table 8. The results are shown in Fig. 9. For both sets of data, a good linear relationship is obtained between the carbon content and the rate constant k_4° in the range of catalysts studied, resulting in

$$k_4^\circ = 1.35 - 0.134\ [\text{wt\% carbon}], \quad \text{UCS} \approx 24.40\ \text{Å} \quad (11)$$

(coefficient of determination = 0.987)

$$k_4^\circ = 1.47 - 0.227\ [\text{wt\% carbon}], \quad \text{UCS} = 24.45\ \text{Å} \quad (12)$$

(coefficient of determination = 0.999), where $2 < \text{wt\% carbon} < 6$. However, it should be kept in mind that two of the samples in the catalysts set with UCS of 24.45 Å are point samples, which were off the correlations developed for the metallic function. Thus, one should be cautious in using Eq. (12). Upon accepting the validity of both the correlations in Fig. 9, an interesting observation can be made. In particular, extrapolating to levels of carbon less than about 1.5 wt%, one can see that the catalysts with the higher UCS exhibit higher acidic function activities in agreement with the results obtained above with the fresh and regenerated samples. However, at carbon contents greater than 1.5 wt% the reverse is observed; catalysts with lower UCS exhibit higher acidic function activities. The activity of sample NU-A with UCS of 24.50 Å also follows this trend, as shown in Fig. 9. This modification in behavior is apparently due to the deposition of coke, which alters the effect of UCS on catalytic activity.

The k_4° values obtained with the samples having a UCS of about 24.40 Å and high as well as low levels of coke, as listed in Tables 8 and 7, respectively, are all shown as a function of wt% C in Fig. 10. Although the two sets of catalysts represent different types of samples, deactivated versus regenerated, an approximate trend that shows k_4° linearly decreasing with wt% C is observed. The corresponding equation is

$$k_4^\circ = 1.64 - 0.194\ [\text{wt\% carbon}], \quad \text{UCS} \approx 24.40\ \text{Å} \quad (13)$$

(coefficient of determination = 0.950), where $0 < \text{wt\% carbon} < 6$. Equation (13) should only be regarded as a preliminary correlation in view of (a) the different types

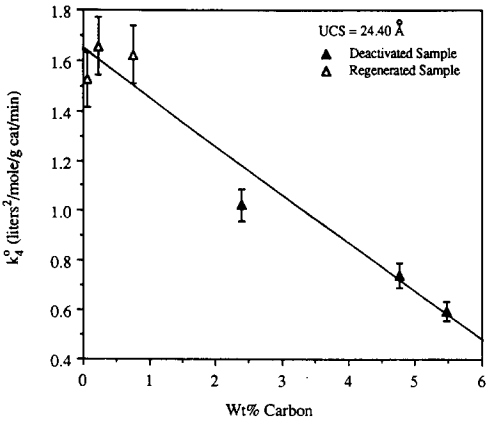

FIG. 10. Plot of k_4° versus wt% carbon for deactivated and regenerated catalysts with unit cell size of about 24.40 Å.

of catalysts used in its derivation and (b) the fact that only a few catalysts were studied.

In the previous work using cumene disproportionation as a probe reaction for the characterization of the acidic function of these hydrocracking catalysts, Absil (*5*) reported that all of the deactivated catalysts with high levels of coke (>2 wt%) had similar activities at a given UCS. This was partially attributed to a reversible poison present on the surface of these deactivated catalysts. Although the exact nature of the poison was not identified, two possible candidates were proposed; (1) reversible or soft coke and (2) nitrogen-containing compounds. The presence of nitrogen-containing compounds on the deactivated catalysts can be readily accounted for, since a typical feed to a commercial hydrocracker contains nitrogen compounds.

Wolf and Alfani (*42*) reviewed the literature dealing with catalyst deactivation by coking and pointed out that Nakano and Kusunoki (*43*) reported two types of coke: (a) volatile or reversible coke and (b) nonvolatile coke. The former is the fraction of coke that is removed from the catalyst surface when purging with hydrogen at reaction temperature. The nonvolatile coke is carbonaceous residue that consists of mono- and polycyclic aromatic rings connected by aliphatic and alicyclic fragments. The relative proportion of each group depends on the reaction-catalyst system used. The groups are interconnected, forming a crystalline pseudographitic structure and an amorphous phase. The degree of crystallinity and cross-linking varies with feed, catalyst, and reaction conditions (*42*). The total volatiles on the deactivated catalysts were determined by Amoco Oil Company and were observed to vary widely (*8*). The exact nature of the poisons on the surface was difficult to assess, since they are strongly dependent on how the catalyst was treated during shutdown and during subsequent handling.

In the present study, the effect due to the reversible poison reported by Absil (*5*) was not observed. If indeed the poison consists of nitrogen-containing compounds adsorbed on the catalyst surface, then these are not expected to result in considerable activity changes since the feed itself used in the present study contains a very basic nitrogen-containing compound. The successful characterization of the deactivated samples in the present work points toward the validity of the above hypothesis.

The Effect of Wt% Carbon on Decay Parameter a_4

The effects of both low and high levels of sulfur and carbon content on the decay parameters a_2, a_3, and a_4 (Eq. (1)) were investigated using the results from the experiments discussed above. No correlation was observed between either wt% S or wt% C and decay parameters a_2 and a_3. Since carbon deposition was indicated above as the primary reason for the deactivation of the acidic function, the estimates of a_4 as a function of wt% carbon for both the regenerated and deactivated catalysts are shown in Fig. 11. The data for the regenerated samples suggest that within experimental error the wt% carbon does not have an effect on the decay parameter. This result is consistent with the shell-progressive combustion model discussed above for these regenerated catalysts. In particular, if the catalysts

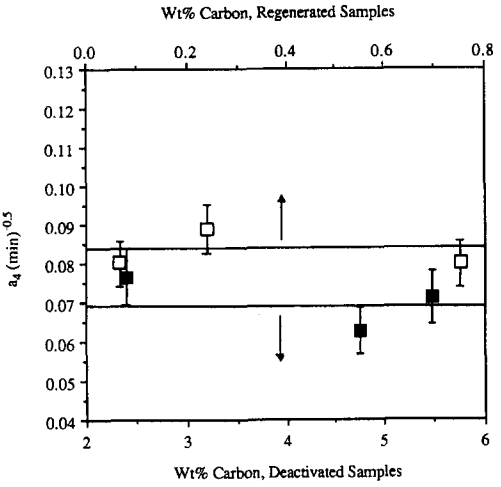

FIG. 11. The effect of catalyst wt% carbon on a_4 for deactivated and regenerated catalysts.

are regenerated under highly diffusion-controlled conditions, then upon grinding the catalyst pellets two types of particles are obtained: (a) coked, inactive particles and (b) active particles. The acidic properties of the active particles should be the same regardless of the fraction of the inactive particles present in the samples, hence the deactivation rate does not show any dependency on wt% carbon. Similar results were reported by Absil (*5*) when examining the decay parameter for cumene disproportionation over regenerated catalysts.

The data for the deactivated samples also suggest no change in the value of a_4 with wt% carbon. Because of the nature of these catalysts a larger experimental error was assigned in the measurements of a_4 (*8*). The reason for the constancy of a_4 with wt% carbon in the deactivated samples is not clear. However, the results could be understood if one assumes that the nature of the acidic sites undergoes a modification when carbon up to about 2 wt% is deposited, but at higher wt% carbon levels no more change occurs in the nature of the sites. The modification in the nature of the sites could involve a reduction in acidity since deactivation rates of the deactivated catalysts were slightly lower than those of the regenerated catalysts.

The Effects of Deactivation and Regeneration on the Hydrocracking Catalyst

To determine the effects of deactivation on the catalyst, the chemical and physical properties of two spent commercial hydrocracking catalysts (NU-B and 3651-171-A) are compared with those of the fresh sample (NU-D) and are listed in Table 9. Once the fresh catalyst is contacted with the industrial feedstock in the commercial hydrocracker, progressive coke deposition occurs on the catalyst surface as indicated by the increase in the wt% carbon after 1 and 2 years on stream. It is expected that the deposition of carbonaceous materials on these catalysts during hydrocracking is responsible for the initial fast decline in catalytic activity. In constant conversion runs, the catalyst temperature must then be increased to maintain conversion. Although a considerable number of studies is reported in the literature concerning the deactivation of dual-functional catalysts in general and especially of those catalysts employed in coal liquefaction operations, only a limited number of investigations have been published on the deactivation of hydrocracking catalysts. There are many similarities, however, in the deactivation by carbonaceous deposits resulting from coal liquids processing, petroleum residue, and heavy oil processing (*44*). The carbon content generally increases

TABLE 9

The Effects of Deactivation on the Chemical and Physical Properties of Catalyst NU-D[a]

Catalyst property	NU-D	NU-B	3651-171-A
Time on stream (years)	0.0	1.0	2.0
C (wt%)	0.03	2.41	5.48
S (wt%)	0.10	2.41	3.56
UCS (Å)	24.56	24.40	24.39
Surface area (m^2/g)	406	211	207
Micropore volume (cc/g)	0.071	0.033	—

[a] Fresh hydrocracking catalyst.

from the entrance to the exit of a fixed-bed reactor. The carbonaceous deposit is usually found to be uniformly distributed throughout the catalyst particles for distillates hydroprocessing. In contrast, it is concentrated at the external surface of the catalyst extrudate for heavy feeds such as asphaltene or preasphaltene. The reaction conditions as well as the feeds used also affect the profile of the deposition of coke. Furthermore, the chemical composition of the deposit depends upon the feedstocks and the operating conditions (*44*).

Many studies have previously concluded that carbon deposition contributes significantly to initial deactivation of typical hydroprocessing catalysts (*45–47*). Of course, it is of paramount interest to directly relate coke formation on various catalysts to their actual deactivation rate or catalytic activity. Kinetics of coking were first analyzed by Voorhies (*11*), while more sophisticated models were recently developed by Beeckman and Froment (*48, 49*). Arteaga *et al.* (*50*) studied the influence of catalyst coke loading on the hydrodesulfurization (HDS) conversion of thiophene using an industrial $CoMo/\gamma\text{-}Al_2O_3$ hydrotreating catalyst, which was subjected to accelerated deactivation by exposure to a 1,3-butadiene stream at 450°C prior to the activity measurements. The thiophene HDS conversion was found to decrease linearly with the wt% coke and the deactivation was almost complete for coke loadings larger than 15 wt%.

Upon deactivation of the hydrocracking catalyst, the surface area decreased as shown in Table 9. This was also observed by Holloway and Nelson (*46*) in the deactivation of $CoMo/SiO_2Al_2O_3$ catalysts in the Synthoil process, by Ocampo *et al.* (*47*) in the deactivation of HDS catalysts in coal liquefaction and by Arteaga *et al.* (*50, 51*) in the deactivation of a commercial $CoMo/Al_2O_3$ catalyst during exposure to a methylcyclopentane stream at 450°C.

Coking results in catalyst deactivation by direct and/or indirect surface suppression. In direct surface suppression the coke precursors are irreversibly adsorbed on the same active sites as those required by the main reaction. Thus, deactivation occurs because of direct abstraction of active sites or active areas from the catalytic cycle. In the case of indirect surface suppression, coke deposition creates a barrier for reactant transport to the active sites. This effect becomes more predominant when extensive coking occurs. Formation of coke deposits near the pore mouths decreases the effective diffusivity and ultimately blocks access to active sites (*42*). Prasher *et al.* (*52*) examined the deactivation of alumina-based hydrocracking catalysts to determine the effect of coke deposition on diffusion parameters. Three catalyst samples were compared; one was the fresh catalyst, while the other two samples were used for hydrocracking of residuum under varying conditions of high temperature and pressure for several days. The results showed that the used pellets exhibited severe reduction in intraparticle diffusion. The deposition of coke on these pellets during reaction resulted in the blocking of pores and also in the reduction of their sizes. Ocampo *et al.* (*47*) compared the pore volume distribution curves for fresh and used coal liquefaction catalysts and found that a significant decline in the pore volume, particularly in the pore size range <3.5 nm, had occurred during the deactivation process. Upon regeneration in air, the pore characteristics of the fresh catalyst were recovered. For the commercial hydrocracking catalyst of the present investigation, the pore volume ($r > 10$ Å) was examined as a function of wt% carbon. Upon coke deposition, the pore sizes were reduced gradually; no evidence of pore plugging was found (*5*). The micropore volume, however, was reduced sharply with wt% carbon as shown in Table 9. This suggests that the smaller pores are blocked or plugged to a greater extent than the larger pores.

Inorganic salts, water, metals, and organic compounds of sulfur, nitrogen, or oxygen present in petroleum act as poisons for

the hydrocracking catalysts (*53*) and can also result in catalyst deactivation. Each of these foreign constituents affects the catalyst in a different way. Sulfur compounds inhibit the metallic component, while nitrogen compounds mainly inhibit the acidic component of the catalyst. The metal contaminants in petroleum are deposited on the catalyst and can promote various dehydrogenation reactions and also increase coke-producing tendency. Oxygen compounds do not pose any serious problem to the refiner, although under certain conditions it has been reported to cause permanent catalyst deactivation (*53*). The organosulfur and organonitrogen compounds in the feed can be effectively removed by employing HDS and hydrodenitrogenation (HDN), respectively (*35*). While a considerable amount of literature has been published on the poisoning of acidic oxides and zeolites by nitrogen compounds, there is even more literature on the poisoning of supported metal catalysts. A large fraction of the literature dealing with the poisoning of metal catalysts is devoted to the interactions of various sulfur compounds with metallic surfaces. A pioneering work on the poisoning of metallic catalysts was carried out by Maxted (*54*) who examined not only sulfur poisons but almost anything with a lone pair of electrons that could bond with a coordinately unsaturated metal. A more recent detailed review by Bartholomew *et al.* (*55*) specifically examined poisoning of metals by sulfur. They concluded that metal–sulfur bonds of adsorbed sulfur are significantly stronger than metal–sulfur bonds in bulk metal sulfides. At low coverages of sulfur on metals, sulfur resides in the high-coordination sites, each sulfur atom bonded to three or four metal atoms. As the sulfur coverage is increased, the surface restructures and in some cases may incorporate metal atoms into the surface sulfur layer. The adsorbed sulfur impurities reduce the capacity of metals for adsorption and reaction of other molecules, which results in a reduction of catalytic activity (*56*).

The data in Table 9 indicate that in commercial use sulfur is progressively deposited on the hydrocracking catalyst after 1 and 2 years on stream. Sulfur deposition can thus be considered as a possible deactivation mechanism for the metallic function of this catalyst. Similar conclusions were reported by Pookote *et al.* (*2*) who studied the effects of commercial use and deactivation on the performance of the same cobalt molybdate hydrocracking catalyst using cyclohexene hydrogenation as a probe reaction. They reported that progressive deposition of sulfur on the catalyst during commercial use affected the net oxidation state of the Mo, and this resulted in a decrease of the hydrogenation activity of the catalyst. The decline in activity was linearly correlated with the wt% sulfur on the catalyst.

An indirect poisoning of the metal is also possible when supported metal catalysts are used. In hydrocracking, the metal hydrogenation components are usually impregnated on acidic supports such as alumina or silica–alumina. Since the metal is intimately associated with the support, adsorption of compounds on the support adjacent to the metal can create a steric blocking that affects the reactions on the metal (*57*). For dual-functional catalysts containing both a metallic and an acidic component, such as those used in hydrocracking, the metal is thought to have a special role (*38*). This role is to prevent irreversible adsorption of coke and coke precursors over the acidic surface. This protection is postulated to extend for a relatively short distance from the metallic sites. It seems possible that the metal sites are a source of hydrogen carriers that are capable of reacting with strongly adsorbed hydrogen-deficient hydrocarbons on the acidic sites. This hydrogen transfer reaction results in a less strongly adsorbed molecule on the acidic sites. Therefore, without the metal present the hydrogen-transfer species do not form and the acidic sites are filled with strongly and irreversibly adsorbed poisons. Similarly, if a poison adsorbs on the metal, it can indirectly result in subsequent adsorption of coke precursors on the acidic

sites (*57*). In conclusion, over dual-functional catalysts four separate cases of poisoning can affect kinetics (*57*): (a) direct adsorption on the acidic sites, (b) direct adsorption on the metallic sites, (c) indirect adsorption on metallic sites–geometric interaction between two kinds of sites, and (d) indirect adsorption on acidic sites–kinetic interaction between metallic and acidic sites.

The decrease in the unit cell size during the deactivation process (Table 9) can be explained as follows. If the unit cell size is assumed to be a measure of the Si/Al ratio of the ultrastable zeolite framework, then the decrease in unit cell size suggests that during the deactivation process, the zeolite is dealuminated. The removal of aluminum from the zeolite requires the presence of either water or ammonia (*29, 31, 58*). Two possible sources of water can be identified. First, since industrial feeds may contain oxygen-containing compounds, as previously mentioned, the latter undergo hydrodeoxygenation to yield water and hydrocarbons. Second, about 5 to 10 wt% physically adsorbed water is present on zeolites. Consequently, during start-up this water is removed as water vapor. The nitrogen-containing compounds present in the feed undergo HDN to yield ammonia and hydrocarbons. The ammonia may react with Brønsted acid sites to form an amidozeolite Y and water (*58*). The water formed in the above cases can undergo reaction with the zeolite resulting in removal of aluminum atoms from the zeolite framework (*29*). At this point, it is not certain which of these are predominantly responsible for dealumination.

The deactivated catalysts were regenerated according to four regeneration techniques described in Table 2. They can be further classified into two categories. In the first category, which includes techniques I and II, the UCS changes during the regeneration process. In techniques III and IV of the second category, the UCS remains constant. Typical examples of both categories

TABLE 10a

The Effects of Regeneration Technique I on the Chemical and Physical Properties of Catalyst NU-B

Catalyst property	NU-B	NU-C
UCS (Å)	24.40	24.35
C (wt%)	2.41	0.21
S (wt%)	2.41	0.24
Surface area (m^2/g)	211	277
Micropore volume (cc/g)	0.033	0.061

TABLE 10b

The Effects of Regeneration Technique IV on the Chemical and Physical Properties of Catalyst 3651-171-A

Catalyst property	3651-171-A	3651-171-B
UCS (Å)	24.39	24.39
C (wt%)	5.48	0.067
S (wt%)	3.56	0.36
Surface area (m^2/g)	207	272

are shown in Tables 10a and 10b. In both of the regeneration techniques the decrease in wt% carbon and wt% sulfur is due to the oxidation of coke to CO, CO_2, and water, and of sulfur to SO_2, respectively. If the UCS is taken as a measure of the Si/Al ratio of the zeolite framework, then to account for the decrease in the UCS, the water formed upon regeneration presumably attacks the zeolite such that aluminum atoms are removed in the form of aluminum oxide/hydroxide clusters (*29, 59*). The water attacking the zeolite can be partly attributed to the geometry of the bed used in the regeneration procedure. In particular, the catalyst bed in the muffle furnace (regeneration technique I) was probably of the deep-bed type, such that water was allowed to remain in contact with the zeolite. If a shallow bed had been used, as in regeneration technique IV, then the water produced would have been removed from the bed before it could attack the zeolite and the UCS would not

have changed during this regeneration process.

It is therefore important, as illustrated above, in the recovery of the zeolite activity during the deactivation–regeneration process, to prevent the water generated via coke oxidation from attacking the zeolite. On a small scale this can be performed by regeneration in a shallow catalyst bed. On a large-scale regeneration technique III (Table 2) can be used. In this particular technique, used commercially to regenerate the hydrocracking catalysts under investigation, the UCS did not decrease during regeneration (*5*). However, the only problem is that the spent catalysts must be removed from the hydrocracker. The above results indicate that although it is desirable to be able to regenerate the commercial catalysts *in situ,* changes in the zeolite UCS should be expected, since the water formed during the regeneration process is then allowed to attack the zeolite framework. Whether such changes in the UCS are important depends highly on the product distribution desired and the process economics.

The loss of metallic function activity during regeneration may be due to a loss of available metal surface (*2*), as discussed earlier. In addition, the high temperature might produce some chemical changes in the metallic sites. It has been reported that calcination of cobalt molybdate on alumina catalysts at high temperatures results in solid–solid reactions leading to changes in the structure and composition of the catalyst (*60*). For example, in $CoMo/Al_2O_3$ catalysts calcined above 600°C, cobalt ions move into the alumina lattice, forming a cobalt aluminate phase which is difficult to reduce. It is also possible that the structural changes occurring at high temperatures may result in partial physical entrapment and thus loss of accessibility of the reducible oxides (*60*). At the temperatures used for regeneration, the amount of MoO_3 lost due to sublimation is probably not significant. Phase identification using X-ray diffraction might be able to verify or eliminate some of the above possibilities (*1*).

CONCLUSION

The results from this study show that changes in the unit cell size of the zeolite component of a commercial hydrocracking catalyst can exert great influence on the reaction rates of a bifunctional reaction system such as piperidine hydrogenolysis. In addition, an inverse relationship between catalyst deactivation and unit cell size is generally observed for both catalyst functions. Thus, zeolite unit cell size is a possible parameter for correlating catalytic activity as well as selectivity, especially for the acidic catalyst function.

The results also show that the sulfur and carbon contents of a hydrocracking catalyst can have a great impact on the reaction rates of the piperidine hydrogenolysis system. In some reactions, the regenerated catalysts exhibit a dependency on sulfur content and possess lower metallic function activity than the fresh sample. This is attributed to a loss of active metal sites during the deactivation–regeneration process and/or to different sensitivities toward sulfur of the various catalyst metal sites. The primary cause of the loss of metallic function activity for the deactivated catalysts is sulfur deposition on the surface. One of the major causes of deactivation for the acidic function is coke deposition. The regenerated catalysts with constant unit cell size and low levels of coke (<0.8 wt%) have similar acidic function activities. These results point to the sulfur and carbon contents as possible parameters for correlating/predicting catalytic activity and selectivity of a commercial hydrocracking catalyst.

In addition, the results of the present investigation are in good agreement with the previous studies on the same hydrocracking catalysts (*1–7*), which were based on separate probings of the two catalyst functions. This suggests that the interactions between the metallic and acidic catalyst functions under reaction conditions, although important,

do not seem to change overall the previously observed dependency of the metallic and acidic function activities on the chemical and physical properties of the catalyst. Furthermore, the present results verify that the probe reaction technique provides information that is generally valid and not simply an artifact of the specific reaction selected.

ACKNOWLEDGMENTS

This research was supported by Amoco Oil Company. We thank R. J. Bertolacini and L. C. Gutberlet of Amoco for the catalyst samples.

REFERENCES

1. Pookote, S. R., Ph.D. dissertation, Northwestern University, Evanston, IL, 1980.
2. Pookote, S. R., Dranoff, J. S., and Butt, J. B., *in* "Proceedings, 7th International Symposium Chem. React. Eng., Boston" (J. Wei, and C. Georgakis, Eds.), Am. Chem. Soc. Symposium Series, Vol. 196, p. 283. Am. Chem. Soc., Washington, DC, 1982.
3. Absil, R. P. L., M.S. thesis, Northwestern University, Evanston, IL, 1982.
4. Absil, R. P. L., Butt, J. B., and Dranoff, J. S., *J. Catal.* **85,** 415 (1984).
5. Absil, R. P. L., Ph.D. dissertation, Northwestern University, Evanston, IL, 1984.
6. Absil, R. P. L., Butt, J. B., and Dranoff, J. S., *J. Catal.***92,** 187 (1985).
7. Absil, R. P. L., Butt, J. B., and Dranoff, J. S., *J. Catal.* **95,** 220 (1985).
8. Hadjiloizou, G. C., Ph.D. dissertation, Northwestern University, Evanston, IL, 1989.
9. Hadjiloizou, G. C., Butt, J. B., and Dranoff, J. S., *J. Catal.* **131,** 545 (1991).
10. Hadjiloizou, G. C., Butt, J. B., and Dranoff, J. S., *J. Catal.* **134** (1992).
11. Voorhies, A., Jr., *Ind. Eng. Chem.* **37**(4), 318 (1945).
12. Pine, L. A., Maher, P. J., and Wachter, W. A., *J. Catal.* **85,** 466 (1984).
13. Breck, D. W., and Flanigen, E. M., "Molecular Sieves," p. 47. Soc. Chem. Ind., London, 1968.
14. Topchieva, K. V., and Huo Shih Thuoang, *Kinet. Katal.***11**(2), 490 (1970).
15. Koradia, P. B., Kiovsky, J. R., and Asim, M. Y., *J. Catal.***66,** 290 (1980).
16. Corma, A., Fornés, V., Montón, J. B., and Orchillés, A. V., *Prepr.-Am. Chem. Soc., Div. Pet. Chem.* **31**(1), 184 (1986).
17. Lombardo, E. A., Gaffney, T. R., and Hall, W. K., *in* "Proceedings, 9th International Congress on Catalysis, Calgary, 1988" (M. J. Phillips and M. Ternan, Eds.), Vol. 1, p. 412. Chem. Institute of Canada, Ottawa, 1988.
18. Arribas, J., Corma, A., Fornés, V., and Melo, F., *J. Catal.* **108,** 135 (1987).
19. Jiao, Q., Jiang, D., Fan, S., and Cao, J., *Gaodeng Xuexiao Huaxue Xuebao* **10**(7), 729 (1989).
20. Gao, Z., Tang, Y., and Zhu, Y., *Appl. Catal.* **56,** 83 (1989).
21. Corma, A., Fornés, V., Montón, J. B., and Orchillés, A. V., *Ind. Eng. Chem. Res.* **26**(5), 882 (1987).
22. Fichtner-Schmittler, H., Lohse, U., Engelhardt, G., and Patzelová, V., *Crystallogr. Res. Technol.* **19**(1), K1 (1984).
23. Desikan, P., and Amberg, C. H., *Can. J. Chem.* **42,** 843 (1964).
24. Satterfield, C. N., Modell, M., and Mayer, J. F., *AIChE J.* **21**(6), 1100 (1975).
25. Yang, S. H., and Satterfield, C. N., *J. Catal.* **81,** 168 (1983).
26. Yang, S. H., and Satterfield, C. N., *Ind. Eng. Chem. Process Des. Dev.* **23**(1), 20 (1984).
27. Kwart, H., Katzer, J., and Horgan, J., *J. Phys. Chem.* **86**(14), 2641 (1982).
28. Rabo, J. A., *Catal. Rev.-Sci. Eng.* **23**(1&2), 293 (1981).
29. Kerr, G. T., *J. Phys. Chem.* **71**(12), 4155 (1967).
30. Kerr, G. T., *J. Phys. Chem.* **72**(7), 2594 (1968).
31. Kerr, G. T., *J. Catal.* **15,** 200 (1969).
32. Jacobs, P. A., Leeman, H. E., and Uytterhoeven, J. B., *J. Catal.* **33,** 31 (1974).
33. Sohn, J. R., DeCanio, S. J., Fritz, P. O., and Lunsford, J. H., *J. Phys. Chem.* **90**(20), 4847 (1986).
34. Corma, A., Fornés, V., Martinez, A., and Orchillés, A. V., *in* "Perspectives in Molecular Sieve Science" (W. H. Flank and T. E. Whyte, Jr., Eds.), Am. Chem. Soc. Symposium Series, Vol. 368, p. 542. Am. Chem. Soc., Washington, DC, 1988.
35. Satterfield, C. N., "Heterogeneous Catalysis in Practice." McGraw–Hill, New York, 1980.
36. Weisz, P. B., and Goodwin, R. D., *J. Catal.* **2,** 397 (1963).
37. Riley, K. L., Silbernagel, B. G., and Butt, J. B., 7th North American Meeting, The Catalysis Society, Boston, MA, October 11–15, 1981.
38. Beuther, H., and Larson, O. A., *Ind. Eng. Chem. Process Des. Dev.* **4**(2), 177 (1965).
39. Franck, J.-P., and Martino, G. P., *in* "Deactivation and Poisoning of Catalysts" (J. Oudar and H. Wise, Eds.), Chemical Industries, Vol. 20, p. 205. Dekker, New York, 1985.
40. Petersen, E. E., *in* "Catalyst Deactivation" (E. E. Petersen and A. T. Bell, Eds.), Chemical Industries, Vol. 30, p. 39. Dekker, New York, 1987.
41. Richardson, J. T., *Ind. Eng. Chem. Process Des. Dev.* **11**(1), 8 (1972).
42. Wolf, E. E., and Alfani, F., *Catal. Rev.-Sci. Eng.* **24**(3), 329 (1982).
43. Nakano, K., and Kusunoki, K., *J. Chem. Eng. Jpn.* **8,** 131 (1975).

44. Nishijima, A., Shimada, H., Yoshimura, Y., Sato, T., and Matsubayashi, N., *in* "Catalyst Deactivation" (B. Delmon and G. F. Froment, Eds.), Studies in Surface Science and Catalysis, Vol. 34, p. 39. Elsevier, Amsterdam, 1987.
45. Kang, C. C., and Johanson, E. S., *Prepr.-Am. Chem. Soc., Div. Fuel Chem.* **21**(5), 32 (1976).
46. Holloway, P. H., and Nelson, G. C., *Prepr.-Am. Chem. Soc., Div. Pet. Chem.* **26,** 1352 (1977).
47. Ocampo, A., Schrodt, J. T., and Kovach, S. M., *Ind. Eng. Chem. Prod. Res. Dev.* **17**(1), 56 (1978).
48. Beeckman, J. W., and Froment, G. F., *Ind. Eng. Chem. Fundam.* **18**(3), 245 (1979).
49. Beeckman, J. W., and Froment, G. F., *Chem. Eng. Sci.* **35,** 805 (1980).
50. Arteaga, A., Fierro, J. L. G., Delannay, F., and Delmon, B., *Appl. Catal.* **26,** 227 (1986).
51. Arteaga, A., Fierro, J. L. G., Grange, P., and Delmon, B., *in* "Catalyst Deactivation" (B. Delmon and G. F. Froment, Eds.), Studies in Surface Science and Catalysis, Vol. 34, p. 59. Elsevier, Amsterdam, 1987.
52. Prasher, B. D., Gabriel, G. A., and Ma, Y. H., *Ind. Eng. Chem. Process Des. Dev.* **17**(3), 266 (1978).
53. Choudhary, N., and Saraf, D. N., *Ind. Eng. Chem. Prod. Res. Dev.* **14**(2), 74 (1975).
54. Maxted, E. B., *in* "Advances in Catalysis" (W. G. Frankenburg, V. I. Komarewsky, and E. K. Rideal, Eds.), Vol. 3, p. 129. Academic Press, New York, 1951.
55. Bartholomew, C. H., Agrawal, P. K., and Katzer, J. R., *in* "Advances in Catalysis" (D. D. Eley, H. Pines, and P. B. Weisz, Eds.), Vol. 31, p. 135. Academic Press, San Diego, 1982.
56. Bartholomew, C. H., *Chem. Eng.* **91**(23), 96 (1984).
57. Larson, O. A., *Prepr.-Am. Chem. Soc., Div. Pet. Chem.* **12,** B-123 (1967).
58. Kerr, G. T., and Shipman, G. F., *J. Phys. Chem.* **72**(8), 3071 (1968).
59. Scherzer, J., *in* "Catalytic Materials: Relationship Between Structure and Reactivity" (T. E. Whyte, Jr., *et al.,* Eds.), Am. Chem. Soc. Symposium Series, Vol. 248, p. 157. Am. Chem. Soc., Washington, DC, 1984.
60. Parekh, B. S., and Weller, S. W., *J. Catal.* **55,** 58 (1978).